Titration Behavior of Residues at the Entrance of the D-Pathway of Cytochrome *c* Oxidase from *Paracoccus denitrificans* Investigated by Continuum Electrostatic Calculations

Elena Olkhova,* Volkhard Helms,† and Hartmut Michel*
*Max Planck Institute of Biophysics, Department of Molecular Membrane Biology, D-60438 Frankfurt, Germany; and †Saarland University, Center for Bioinformatics, 66041, Saarbrücken, Germany

ABSTRACT Continuum electrostatic calculations were employed to investigate the titration curves of the fully oxidized state of wild type and several variants of cytochrome *c* oxidase from *Paracoccus denitrificans* (N131D, N131C, N131V, and D124N) for different values of the dielectric constant of the protein. The effects of the mutations at the entrance of the D-proton transfer pathway were found to be quite localized to their immediate surroundings. The results can be well interpreted in the light of the available biochemical and structural data and help understanding the effects of mutations on proton conductivity. The mutations of aspartic acid Asp-I-124 to a neutral residue resulted in a decreased pK_a value of His-I-28 suggesting that the mutation of His-I-28 may have a significant influence on the coupling of electron and proton transfer in cytochrome *c* oxidase. We also investigated the effect of the mutations N131D, N131C, and N131V on the residue Glu-I-278 in terms of its pK_a value and electrostatic interaction energies.

INTRODUCTION

During the past decades, intense experimental and theoretical efforts have been devoted to unraveling the function and mechanism of coupled electron and proton transport in cytochrome *c* oxidase (COX) that catalyzes the terminal step in cellular respiration, a four-electron transfer from cytochrome *c* to dioxygen, in the inner membrane of mitochondria and many bacteria (1,2). The four protons required for the reduction of dioxygen to water are provided from the internal space of mitochondria or bacteria. In addition, four protons are translocated across the inner mitochondrial membrane or the bacterial cytoplasmic membrane (3). As a result, eight elementary charges are transferred across the membrane during the catalytic cycle. A wealth of information is available on the structural and functional properties of cytochrome *c* oxidases from crystal structure determinations (4–7) and various spectroscopic, biochemical, and theoretical studies.

Based on the x-ray structures of COX from different organisms and in agreement with the results of site-directed mutagenesis studies (8–16), two possible proton transfer pathways have been suggested (4). The shorter one, referred to as the K-pathway, leads to the binuclear center via the highly conserved residues Lys-I-354, Thr-I-351, and Tyr-I-280 (numbering for the COX from *Paracoccus denitrificans*). The second, longer pathway (D-pathway) involves Asp-I-124 and a number of conserved polar residues, and leads to residue Glu-I-278 via a water-filled cavity. The current view is that these two proton transfer pathways are associated with different parts of the catalytic cycle. Whereas Asp-I-124 was previously identified as a likely proton entry site for the D-pathway, Glu-78 from subunit II (Glu-II-78) was proposed as the likely entry site of the K-pathway on the basis of electrostatic calculations (17). This proposal has been confirmed by site-directed mutagenesis studies for the enzyme from *Rhodobacter sphaeroides* and the cytochrome *bo* ubiquinol oxidase from *Escherichia coli*, but ironically not for the COX of *P. denitrificans* (18,19). Despite recent advances (5,7), the coupling of proton transfers to the redox processes in COX is largely unknown. The availability of a new crystal structure of a mutant enzyme in which Asp-I-131 close to the entrance of the D-pathway had been replaced by an asparagine (N131D variant structure) permitted us to address the question of how an additional potentially negatively charged residue introduced in the entrance of the D-pathway can influence proton pumping in the enzyme.

The determinations of the crystal structures of COX from *P. denitrificans* (5), from bovine heart (6), and from *Rh. sphaeroides* (7) have provided the positions of a number of water molecules in the D- and K-pathways. These water molecules are likely involved in proton transport along these pathways. Due to the formation of several hydrogen bonds their occupancies are high and their mobilities low enough that they could be distinguished from the background even at resolutions of ~2.5–2.7 Å. However, there is a considerable amount of empty space left in the protein, and in the proton pumping pathways in particular, which should contain less well-ordered water molecules. Therefore, hydration in these pathways has also been investigated in a number of theoretical studies to predict the locations of additional solvation sites (20–25).

Electrostatic interactions play an important role in the processes of proton transfer and generation of transmembrane potential in different membrane proteins (see for review Lancaster

Submitted February 28, 2005, and accepted for publication July 7, 2005.

Address reprint requests to Volkhard Helms, University of Saarland, Center of Bioinformatics, Postfach 15 11 50, 66041, Saarbrücken, Germany. Tel.: 49-681-302-64165; Fax: 49-681-302-64180; E-mail: volkhard.helms@bioinformatik.uni-saarland.de.

© 2005 by the Biophysical Society

0006-3495/05/10/2324/08 $2.00

doi: 10.1529/biophysj.105.062091

(26)). The Poisson-Boltzmann equation of continuum electrostatics describes electrostatic interactions in a multiple dielectric environment of the molecular system (27). The electrostatic potential inside and outside of a macromolecule is computed taking into account the protein atoms represented as partial atomic charges at the centers of spheres filled by an ''internal'' dielectric constant, the solvent that fills all cavities inside the protein and surrounds the protein represented by a (usually higher) different dielectric constant, and the effect of ionic strength modeled by a Debye-Hückel treatment. A cluster of 18 strongly electrostatically interacting titratable groups was previously identified in *P. denitrificans* COX (17). Many residues of the cluster are calculated to be fully charged at pH 7.0 in the fully oxidized state of enzyme despite being buried within the transmembrane part of the protein. Among the few exceptions are the two strongly coupled groups Asp-I-399 and a neighboring heme a_3 propionate that apparently share a single proton, and the neutral Glu-I-278, the acidic function of which has been shown to be crucial for enzyme activity (28). The finding that Lys-I-354 is neutral (17) has been questioned recently because water molecules hydrogen bonded to the homologous residue Lys-I-362 and to Ser-I-299 were found in the *Rh. sphaeroides* COX structure (7). This observation has led to the postulate that the Lys-I-362 may be protonated at pH = 7.0 (*Rh. sphaeroides* numbering). Popović and Stuchebrukhov (29,30) have recently presented pK_a calculations for active site residues from bovine heart COX during different states of the catalytic cycle of the enzyme. They predict a change of the protonation states of His-I-291 (which is one of the ligands of Cu_B) along the catalytic cycle of COX. In that work, focus was placed on the active site residues and few results for the other parts of the protein were shown. Another study presented a free energy profile for coupled electron/proton transfer between Glu-I-278 past the binuclear center (31). These authors concentrated on the catalytic center of the enzyme as well.

The value used for the dielectric constant of proteins is a subject of ongoing intense discussion (see for review Lancaster (26)). An effective dielectric constant of 4 was estimated from molecular dynamics (MD) simulations for several proteins (32) by calculating the fluctuations of the protein dipole moment. The value of the protein dielectric constant calculated in this way strongly depended on how much of the protein was included in the dipole moment fluctuations. Consistent with this findings, the agreement with experimentally measured pK_a values could be significantly improved by increasing the dielectric constant of the protein to 20 (33–36). In addition, several groups (37,38) have argued that the dielectric constant in a protein should be considered variable because it depends on which degrees of freedom in a protein are treated explicitly and which ones are allowed to relax structurally.

The aim of this work is to investigate the sensitivity of the results in the COX system to empirical dielectric parameters, and to clarify the effects of protein mutations in the proton conduction pathways on the titration states of nearby residues.

METHODS

Coordinates and structures used in the calculations

The starting configuration of the fully oxidized two-subunit COX from *P. denitrificans* at 2.7-Å resolution was taken from Protein Data Bank entry post-1AR1. The coordinates of the COX variant N131D used in the calculations are the results of a recent x-ray structure determination (K. L. Dürr, O.-M. H. Richter, P. Hellwig, B. Ludwig, H. Müller, J. Koepke, G. Peng, and H. Michel, unpublished data). They are very similar to the coordinates of wild-type enzyme. Models for the COX variants N131C, N131V, and D124N were created by introducing the appropriate residue using InsightII (Accelrys, San Diego, CA) and the VMD package (39) and subsequent energy minimization. Therefore, a proper membrane environment of the wild-type COX and of the mutant structures was provided by embedding the protein in an equilibrated dimyristoylphosphatidylcholine lipid bilayer taken from Olkhova et al. (25). The minimizations were carried out according to the setup of the system described in Olkhova et al. (25). The microscopic system consisted of COX (two subunits of 549 and 252 amino acids, respectively), the Cu_A metal center, heme *a*, the heme a_3–Cu_B binuclear center including two nearby internal crystal waters and one OH^- molecule. The conformation of each mutant structure was energy minimized using the academic version c28b2 of the biomolecular simulation package CHARMM (40). The protein atoms were initially fixed, only relaxing the remaining system by 100 steps of steepest descent followed by 100 steps of adopted basis Newton-Raphson minimization. When relaxing the protein, a number of energy restraints were used to ensure a smooth relaxation of the system toward an equilibrated configuration (41). Therefore, in the next stage of 100 steps, a harmonic potential of 10 kcal mol^{-1} $Å^{-2}$ was applied to the backbone atoms of the protein. In the last stage of 100 steps, the protein and water constraints were decreased to 5 kcal mol^{-1} $Å^{-2}$ and were gradually reduced to obtain a free system. The only remaining constraints were those on lipid headgroups (25) and harmonic distance restraints between Cu_B and its ligands His-I-276, His-I-325, His-I-326, OH^- and Cu_B, OH^- and the Fe atom of heme a_3, the Fe atom of heme a_3 and His-I-411, the Fe atom of heme *a* and His-I-413, the Fe atom of heme *a* and His-94, Cu_A, and Cys-II-220, Cu_A(I) and His-II-181, Cu_A and Cys-II-216, Cu_A and Met-II-227, Mg and Glu-II-78, Mg and His-I-403, and Mg and Asp-I-404 (25). During the minimization, the backbone atoms of the proteins did not show significant movement. Noticeable reorientations only occurred for some side-chain atoms on the surface of the protein.

Electrostatics calculations

Charges on the protein atoms and ionizable groups in different protonation states were taken from the CHARMM 22 force field (42,43). Partial atomic charges for protonated Asp-I-399 as well as for protonated Glu-I-278 were taken from the AMBER96 force field. Partial atomic charges for heme *a* and heme a_3 sites, the His-I-276 to Tyr-I-280 cross-link, for Cu_B and its three histidine ligands (His-I-276, His-I-325, His-I-326), and for the Cu_A metal center for the fully oxidized state of the catalytic cycle were taken from Olkhova et al. (25).

In our calculations water-filled cavities were treated as a high-dielectric continuum thus neglecting the charge-stabilizing effect of highly directed hydrogen bonds to bound water molecules. Hence, the calculated protonation states for two residues that both point into large water-filled cavities may be artificial due to the limitations of the computer model (17). The regions occupied by explicit water molecules were treated as ''protein'' as far as the dielectric model is concerned.

The finite difference linearized method was used to solve the Poisson-Boltzmann equation. The solvent dielectric constant was set to 78.5 and the protein dielectric constant was set to be 4 or 8.5 or 15 with an ionic strength of 150 mM (36). Atomic radii were scaled by 1.122 to correspond to the radii at the minimum in the Lennard-Jones potential. Hydrogen atom radii were set to zero. The dielectric boundary was positioned at the molecular surface using a probe radius of 1.0 Å with CHARMM 22 atomic radii. Molecules were surrounded by a 2.0-Å-thick ion exclusion layer. The potential at the boundary of the grid was assigned assuming each protein atom is a Debye-Hückel sphere (44). The electrostatic potentials were calculated by means of electrostatic potential grid focusing in four steps. For each of the titratable residues, four cubic grids with spacing of 2.5, 1.2, 0.75, and 0.25 Å and dimensions of 60, 25, 20, and 20 (45), respectively, were used.

pK_a calculations

The method used for calculating electrostatic energies and pK_a values was outlined by several groups (33,36,38,46,47). The pK_a values of all ionizable groups of a protein are estimated by solving the multiple titration site problem at a range of pHs by assuming that the pK_a of an ionizable group at a chosen pH is given by:

$$pK_a = pH - (ln([I]/[HI]))/2.303,$$

where *HI* represents the protonated form and *I* the unprotonated form of the ionizable group. The average value of the pK_a of each ionizable group over the pH range was then computed.

The program UHBD (version 5.1) (48) was used to perform these calculations together with protocols previously employed for pK_a calculations (Demchuk and Wade (36)). These calculations employ the ''single-site'' cluster methodology that is implemented in UHBD scripts (34,35,49) (kindly provided by Dr. R. C. Wade). As an estimate of pK_a (model), the following experimental pK_a values of small compounds in solution were used: Asp, 4.0; Glu, 4.4; Lys, 10.4; Arg, 12.0; His, 6.3; Cys, 8.3; C-terminus, 3.8; N-terminus, 7.5; and 9.6 for Tyr (33). Note that we did not use the *Zrf* criterion (36) because these values were optimized for the OPLS parameters. Ionization of these residues was modeled according to the ''single-site method'' by ionizable sites at pH = 7 located at the position of the CG atom in Asp, the CE atom in Arg, the C atom in the C- terminus, the SG atom in Cys, the CD atom on Glu, the NE atom at the N-terminus, the OG atom in Tyr, and the ND1 and NE2 atoms in His.

RESULTS AND DISCUSSION

Titration states of residues in pathways involved in proton pumping

Fig. 1 shows a sketch of the titratable residues in the D- and K-pathways in COX from *P. denitrificans*. Table 1 lists the computed pK_a values of important residues in the D- and K-pathways where the difference between model pK_a and computed pK_a at an ε of 8.5 exceeds 2 pK_a units. In general, the computed values are in good agreement with those given by Kannt et al. (17) at a $\varepsilon_{prot} = 4$. Unless otherwise indicated, the further discussions always refer to $\varepsilon_{prot} = 8.5$ values.

Focusing on the residues at the entrance of the D-pathway, we notice that the pK_a of His-I-28 is shifted to a relatively low value of 3.5 when the protein dielectric constant is set to a value of 8.5, and to a pK_a of 4.7 when the protein dielectric constant is equal to 15. This result can be understood in the context of the crystal structure because the His-I-28:NE2 atom points into a hydrophobic cavity. Therefore, double

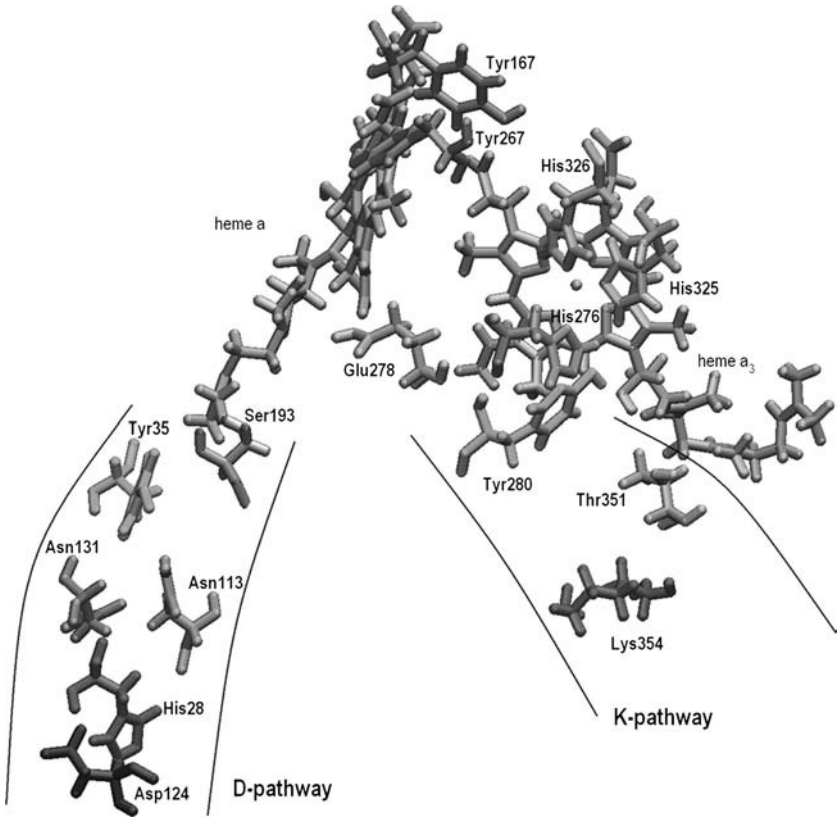

FIGURE 1 Schematic view of amino acids lining the D- and K-proton transfer pathways in subunit I of the cytochrome *c* oxidase from *P. denitrificans*.

TABLE 1 Outcome with different dielectric constants for pK_a calculations: the results for the D- and K-proton transfer pathways in cytochrome *c* oxidase from *P. denitrificans*

Name of residue	pK(model)	$\varepsilon_{prot} = 4$	$\varepsilon_{prot} = 8.5$	$\varepsilon_{prot} = 15$
His-I-28	6.3	0.5	3.5	4.7
Asp-I-30	4.0	1.7	2.1	2.3
Tyr-I-35	9.6	21.7	15.6	12.5
Arg-I-54	12.0	14.6	13.6	13.4
Asp-I-124	4.0	3.2	3.2	3.2
Arg-I-129	12	7.9	9.2	9.9
Tyr-I-135	9.6	15.8	12.3	10.9
Tyr-I-167	9.6	15.8	14.0	13.3
Tyr-I-267	9.6	23.5	20.5	15.5
Glu-I-278	4.4	18.4	15.6	10.4
Tyr-I-280	9.6	22.0	19.1	14.6
His-I-325	6.3	8.5	8.8	8.0
Lys-I-354	10.4	1.0	6.1	8.0
Asp-I-399	4.0	11.1	7.0	6.3
Glu-II-78	4.4	6.3	4.0	3.3
Lys-II-191	10.4	8.1	11.7	12.3
heme *a* propionate PAA	4.8	11.2	8.6	8.8

protonation of His-I-28 would be quite difficult and only becomes favorable at low pH values (Fig. 2). The His-28:ND1 atom is involved in a tight hydrogen bond with the nearby Asp-I-124:OD1 and must consequently always be protonated. The pK_a of Asp-I-124 was computed at a slightly lowered pK_a of 3.2, possibly because only OD2, but not OD1, could carry the proton in this environment.

Asp-I-124 is located at a distance of 8.2 Å from Asp-I-30 (measured between their oxygen atoms). This close interaction will mutually increase their pK_a values as well as reduce the repulsion of the negatively charged unprotonated forms.

We conclude that residues Asp-I-124, His-I-28, and Asp-I-30 form a tightly coupled cluster at the entrance of the D-pathway. The importance of the latter two residues still has to be checked by site-directed mutagenesis.

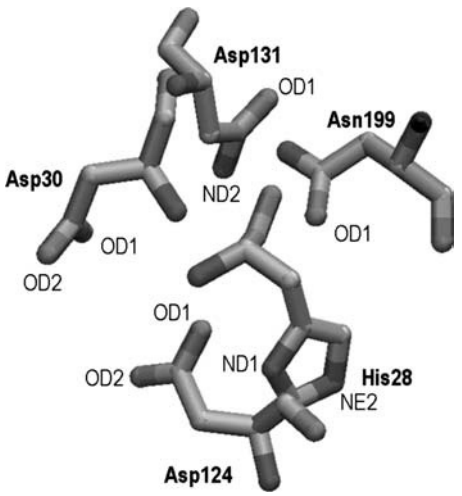

FIGURE 2 All-atom representation of selected residues in cytochrome *c* oxidase around Asn-I-131.

Effect of mutations of Asn-I-131

Residue Asn-I-131, located in the D-pathway, is thought to be important for the formation of the hydrogen bonding network and for the stabilization of the positions of water molecules in this proton transfer pathway (16). As seen in the crystal structure, residue Asn-I-131 forms direct hydrogen bonds with high occupancies toward Tyr-I-135 and Asn-I-113 and a water molecule. In our previous molecular dynamics simulations, we determined the average number of solvent sites in the protein conducting K- and D-pathways, and identified the highly fluctuating hydrogen bonding network, combined with a significant diffusion of individual water molecules. These simulations showed that Asn-I-131 interacts via a water molecule with Thr-I-25 and Asp-I-124 (25). Therefore, Asn-I-131 seems to be a key residue for the formation of the hydrogen bonding network between the entrance of the D-pathway and other residues that are involved in the proton transfer process. To investigate the energetic consequences of the mutations N131D, N131C, and N131V of cytochrome *c* oxidase from *P. denitrificans* ((16) and K. L. Dürr, O.-M. H. Richter, P. Hellwig, B. Ludwig, H. Müller, J. Koepke, G. Peng, and H. Michel, unpublished data), we here complement these studies with electrostatic calculations for these variants.

The replacement of Asn-I-131 by the hydrophobic amino acid valine leads to a complete inactivation of proton pumping, but at the same time severely diminishes the turnover of the mutant enzyme to 6% (16). It is generally difficult to distinguish direct effects of such mutations, i.e., proton transfer is blocked because the mutated residue cannot participate in the transfer chain anymore, from indirect effects by destabilizing nearby internal water molecules or by electrostatic interaction with proton-transferring residues. Our pK_a calculations on the N131V variant show an upward shift of the computed pK_a values of residue Asp-I-124 (from 3.15 to 3.85) and of His-I-28 (from 0.45 to 0.77). Table 2 lists the computed pK_a values of nearby residues for all mutant proteins. Concerning proton transfer, the side chain of the Val-I-131 variant clearly is unable to form any hydrogen bonds and to directly participate in proton transfer in the D-pathway. On the other hand, the asparagine side chain has a high pK_a for deprotonation of ~17. This property would speak against the direct participation of residue 131 in the proton transfer and favor indirect effects. In the case of the N131C variant, similar pK_a variations are observed as for N131V, meaning that all computed pK_a values are similar to those found for the wild-type enzyme with the exceptions of His-I-28 and Asp-I-124 where increases of 0.4 and 0.7 pK_a units, respectively, are predicted. In the ''single-site'' methodology used here, the effect of ionization is modeled by addition or removal of a unit charge change on a single atom in the amino acid side chain. This is a well-tested and robust methodology (50) but may be most suitable for studying the effect of charged mutations (neutral to charged and vice versa). When exchanging neutral

TABLE 2 pK_a values computed for the nearby residues for wild-type cytochrome *c* oxidase and for D124N, N131D, N131V, and N131C variants

	ε_{prot}	His-I-28	Asp-I-30	Tyr-I-35	Residue-I-124	Residue-I-131
Wild type	4	0.5	1.7	ND*	3.2	–
	8.5	3.5	2.1	15.6	3.2	–
	15	4.7	2.3	12.5	3.2	–
D124N	4	−3.1	0.9	ND*	–	–
	8.5	1.5	1.6	15.2	–	–
	15	3.4	1.8	12.3	–	–
N131D	4	1.0	1.8	ND*	4.1	13.4
	8.5	4.4	2.6	15.6	4.6	8.0
	15	5.5	2.8	13.2	4.4	5.7
N131V	4	0.8	1.7	ND*	3.9	–
	8.5	3.7	2.2	15.0	3.6	–
	15	4.8	2.3	12.2	3.4	–
N131C	4	0.9	1.8	ND*	3.9	22.2
	8.5	3.7	2.2	15.1	3.6	13.6
	15	4.9	2.4	12.2	3.4	10.7

*ND, nondefined value.

against neutral residues, the ''full-group method'' (35) may give a finer description of the detailed effects of pK_a predictions. In this method, the addition or removal of a net charge is modeled by redistributing the partial charges over the entire group.

In experiments, the mutation of Asn-I-131 to Asp shows dramatic consequences on the catalytic properties of the enzyme (16,51). In *Rh. sphaeroides* this nonpumping variant had a two times higher steady-state activity than the wild-type enzyme and did not show any proton pumping (52). In *P. denitrificans* the turnover of the N131D variant is comparable to the wild-type enzyme, and proton pumping is negligible. Therefore, the N131D variant can be considered as being truly decoupled (16). The use of different dielectric constants produced quantitatively different results (pK_a values of Asp-I-131 varying from 13.4 to 5.7; see Table 2). For protein dielectric constants of 4 or 8.5, the introduced aspartic acid showed a pK_a value higher than 7 and is thus to be considered as protonated. When the protein dielectric constant is set to a value of 15, the pK_a of Asp-I-131 is computed to be lower than 7. The protonated form of Asp-I-131 (which is present to ~0.5% extent at pH 6 when its pK_a is 8.0) could in principle be transiently directly involved in proton transfers by quickly releasing a proton on one side and accepting one from the other side. However, the wild-type residue Asn-I-131 is involved in an extremely tight hydrogen bonding network (25) that should also extend to the variant enzyme.

Supporting these considerations, the determination of the crystal structure of the N131D variant (K. L. Dürr, O.-M. H. Richter, P. Hellwig, B. Ludwig, H. Müller, J. Koepke, G. Peng, and H. Michel, unpublished data) shows no significant changes in the protein structure compared to the wild-type COX. Consequently, the polar side chains of the aspartic acid or asparagine side chains will be in similar environments with regard to factors such as polarity and exposure to solvent. However, the neighboring side chains will experience different Coulombic interactions due to this potentially negatively charged residue at the entrance of the D-proton transfer pathway for the N131D variant. According to Table 2, the pK_a values of His-I-28, Asp-I-30, Tyr-I-35, and Asp-I-124 are upshifted by 0.5–1.5 pH units. For example, our calculations show the important influence of the N131D mutation on the pK_a value of Asp-I-124. This residue, as the entry point of the D-pathway, has been shown to be a key residue for proton pumping (8,10,12). In the N131D variant, its pK_a increased from 3.15 to 4.1 ($\varepsilon_{prot} = 4$), from 3.2 to 4.6 ($\varepsilon_{prot} = 8.5$), and from 3.2 to 4.4 ($\varepsilon_{prot} = 15$). The large shift of the pK_a value of Asp-I-124 is not surprising because the separation between position I-131 and Asp-I-124 is only 6.7 Å.

Effects on Glu-278

Glu-I-278 is an important residue at the end of the D-proton transfer pathway. It may function as a possible conformational switch to either direct protons toward the heme a_3 propionate group or to conduct them to the binuclear center (4). The connection between the conformational states of Glu-I-278 and the redox state of the enzyme is not clear. In our previous MD simulations for the COX in a fully oxidized state such a conformational change of the protonated Glu-I-278 was not observed and a connection between the protonated Glu-I-278 and the O1A propionate group of heme a_3 was not detected. However, an additional short MD simulation of COX in a fully oxidized state with a deprotonated Glu-I-278 (E. Olkhova, V. Helms, and H. Michel, unpublished data) shows a significant reorientation of the side chain of Glu-I-278 and the formation of a hydrogen bond chain between Glu-I-278 via water molecules up to the O1A atom of the heme a_3 propionate. This difference is thought to be of interest for routing protons in different parts of the catalytic cycle. Although the effect of mutations at the entrance of the D-pathway on the charge-charge interaction with Glu-I-278 are rather small (see Table 3), Table 4 shows significant differences in charge-charge interaction energies between Glu-I-278 and several selected residues for wild-type cytochrome *c* oxidase between the crystallographically observed orientation and the alternative orientation of the side chain of Glu-I-278 (Fig. 3) modeled by MD simulation. The influence of the protein flexibility is again incorporated in a very approximate way via the dielectric constant assigned to the protein interior. The largest difference is found for Tyr-I-267, which is located close to the heme's propionates. Interestingly, this tyrosine residue and Tyr-I-167 have been suggested as candidates of a putative radical species (53).

The space between Glu-I-278 and the binuclear center/heme a_3 propionate group has also been proposed to be a part

TABLE 3 Charge-charge interaction energies (in kcal/mol) for several selected residues of wild-type cytochrome *c* oxidase and several mutants (dielectric constant of protein is 4)

		Wild type	N131D	N131C	N131V	D124N
His-I-28	Res-I-131	ND*	−3.37	−3.35	ND	ND
Res-I-124	Res-I-131	ND	4.43	4.07	ND	ND
Glu-I-278	Res-I-131	ND	1.25	1.37	ND	ND
His-I-28	Glu-I-278	−0.45	−0.45	−0.45	−0.45	−0.45
Res-I-124	Glu-I-278	0.30	0.30	0.30	0.30	ND
His-I-28	Res-I-124	−6.39	−6.39	−6.39	−6.39	ND

*ND, nondefined value.

of the oxygen diffusion channel (4,7,54), which is hydrophobic and does not contain any crystallographically identifiable water molecules. Hydration in this area has been investigated in a number of theoretical studies to predict the locations of additional water molecules (20–25). Glu-I-278 was previously identified to belong to a cluster of 18 strongly interacting residues by Kannt et al. (17). Among the residues listed in our Table 4, only Asp-I-404 belongs to this cluster.

In general, the effects of N131V, N131C, and N131D on Glu-I-278 are computed to be very small in terms of pK_a and interaction energies. For the wild-type enzyme, the pK_a value of Glu-I-278 is computed to be 18.4 when the protein dielectric constant is set to 4. When the dielectric constant is increased to $\varepsilon_{prot} = 8.5$, the pK_a of Glu-I-278 decreases to 15.6. Once the additional negative charge of the Asp-I-131 is present, the pK_a value of Glu-I-278 is shifted upward very slightly (from 15.6 for the wild-type enzyme to 15.7 for the N131D variant). Although these effects can be considered as rather small, they are at variance with the interpretations of experimental results by Namslauer et al. (51), who attributed the lack of proton pumping in the N131D variant to the change of the pK_a of Glu-278 caused by the introduction of the negative charge by the N131D mutation. If the observed absence of proton pumping in the N131D variant is purely attributed to Glu-I-278, one may also consider an effect of the D-pathway mutations on the conformational equilibrium of

TABLE 4 Charge-charge interaction energies (in kcal/mol) between Glu-I-278 and several selected residues (dielectric constant of protein is 4)

	N131D	N131D ALT278
Tyr-I-35	3.24	3.16
Tyr-I-93	1.24	1.35
His-I-94	−2.51	−2.29
Asp-I-131	1.25	1.14
Tyr-I-138	2.68	2.46
Tyr-I-167	2.15	2.73
Tyr-I-267	2.90	3.69
His-I-276	−3.45	−3.07
Tyr-I-280	2.95	2.58
His-I-325	−2.92	−2.82
His-I-403	−1.60	−1.71
Asp-I-404	1.37	1.44
OH^-	3.59	3.35

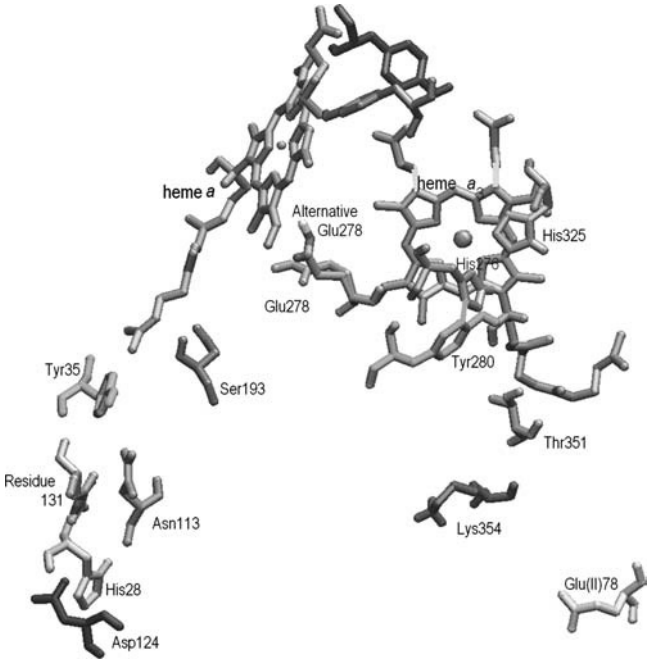

FIGURE 3 Glu-I-278 in the crystallography observed orientation and in an alternative orientation of the side chain of Glu-I-278 and several selected residues in the D- and K-proton transfer pathways.

Glu-I-278 rather than on its explicit titration behavior. As mentioned above, the hydrogen bonding network, including the positions of water molecules from the x-ray structure in the D-pathway (K. L. Dürr, O.-M. H. Richter, P. Hellwig, B. Ludwig, H. Müller, J. Koepke, G. Peng, and H. Michel, unpublished data), is altered by introducing an acidic residue at position 131.

Effect of D124N mutation

To assess the electrostatic contribution of residue D-I-124 on the stability of the hydrogen bonded network in COX we calculated the pK_a values of all titratable residues in this variant. As mentioned before, Asp-I-124:OD1 is engaged in a strong hydrogen bond with His-I-28:ND1 (distance 3.73 Å). Its other carboxyl oxygen Asp-I-124:OD2 points into solution. Upon mutating D124N, we observe a slight outward swing of the side chain of Asp-I-124 away from His-I-28 (distance between His-I-28:ND1 and Asn-I-124:OD1 is 3.81 Å). As mentioned above, Asp-I-124 also has an important influence on the pK_a value of His-I-28. The calculations with different internal dielectric constants indicated that the pK_a value of His-I-28 decreased by 2.7 pK_a units, and at the same time a large decrease in the enzyme activity is observed (Pfitzner et al. (16)). Considering the interaction with Glu-I-278, the COX variant D124N has a smaller effect than N131D, which can simply be attributed to the fact that Glu-I-278 is further away from Asp-I-124 than Asp-I-131. Asp-I-124 is located near Asp-I-30 (distance 8.2 Å). Their mutual

interaction will increase their pK_a values to reduce the eventual repulsion of negative charges. This argument explains why the pK_a of Asp-I-30 is even smaller for the D124N variant (0.9 vs. 1.7 in Table 2).

CONCLUSIONS

For the first time, results from electrostatic continuum calculations are presented for variants of cytochrome *c* oxidase. The effects of two mutations at the entrance of the D-pathway were found to be quite localized to their immediate surroundings. Residues Asp-I-124, His-I-28, and Asp-I-30 form a tightly coupled cluster at the entrance of the D-pathway. The importance of the residues His-I-28 and Asp-I-30 has to be determined by site-directed mutagenesis. Our calculations demonstrate the important influence of the N131D mutation on the pK_a value of Asp-I-124. The effects of N131V, N131C, and N131V mutations on Glu-I-278 are computed to be very small in terms of pK_a values and interaction energies. They are at variance with the interpretations of recent experimental results and require further investigations.

The authors thank Dr. Rebecca Wade (European Media Lab Research GmbH, Heidelberg, Germany) for the provision of several scripts for computing pK_a values from UHBD calculations and Dr. Jürgen Koepke for sharing the coordinates of the so far unpublished crystal structure of the N131D mutant. E.O. is grateful to Barbara Schiller for the computational support and to Dr. Stephen Marino and Elena Herzog for the critical reading of manuscript.

This work was supported by the Deutsche Forschungsgemeinschaft (SFB 472), the Fonds der Chemischen Industrie, and the Max-Planck-Gesellschaft.

REFERENCES

1. Ferguson-Miller, S., and G. T. Babcock. 1996. Heme/copper terminal oxidases. *Chem. Rev.* 96:2889–2908.
2. Michel, H. 1998. The mechanism of proton pumping by cytochrome c oxidase. *Proc. Natl. Acad. Sci. USA.* 95:12819–12824.
3. Wikström, M. K. F. 1977. Proton pump coupled to cytochrome *c* oxidase in mitochondria. *Nature.* 266:271–273.
4. Iwata, S., C. Ostermeier, B. Ludwig, and H. Michel. 1995. Structure at 2.8 Å resolution of cytochrome *c* oxidase from *Paracoccus denitrificans*. *Nature.* 376:660–669.
5. Ostermeier, C., A. Harrenga, U. Ermler, and H. Michel. 1997. Structure at 2.7 Å resolution of the *Paracoccus denitrificans* two-subunit cytochrome *c* oxidase complexed with an antibody F_V fragment. *Proc. Natl. Acad. Sci. USA.* 94:10547–10553.
6. Tshukihara, T., H. Aoyama, E. Yamashita, T. Tomizaki, H. Yamaguchi, K. Shinzawa-Itoh, R. Nakashima, R. Yaono, and S. Yoshikawa. 1996. The whole structure of the 13-subunit oxidized cytochrome *c* oxidase at 2.8 Å. *Science.* 272:1136–1144.
7. Svensson-Ek, M., J. Abramson, G. Larsson, S. Tornroth, P. Brzezinski, and S. Iwata. 2002. The X-ray crystal structures of wild-type and EQ (I-286) mutant cytochrome *c* oxidases from *Rhodobacter sphaeroides*. *J. Mol. Biol.* 321:329–339.
8. Thomas, J. W., A. Puustinen, J. O. Alben, R. B. Gennis, and M. Wikström. 1993. Substitution of asparagine for aspartate-135 in subunit I of the cytochrome *bo* ubiquinol oxidase of *Escherichia coli* eliminates proton-pumping activity. *Biochemistry.* 32:10923–10928.
9. Fetter, J. R., J. Quian, J. Shapleigh, J. W. Thomas, J. A. Garcia-Horsman, E. Schmidt, J. Hosler, G. T. Babcock, R. B. Gennis, and S. Ferguson-Miller. 1995. Possible proton relay pathways in cytochrome *c* oxidase. *Proc. Natl. Acad. Sci. USA.* 92:1604–1608.
10. Garcia-Horsman, J. A., A. Puustinen, R. B. Gennis, and M. Wikström. 1995. Proton transfer in cytochrome bo_3 ubiquinol oxidase of *Escherichia coli*: second-site mutations in subunit I that restore proton pumping in the mutant Asp-135 → Asn. *Biochemistry.* 34:4428–4433.
11. Hosler, J. P., J. P. Shapleigh, D. M. Mitchell, Y. Kim, M. A. Pressler, C. Georgiou, G. T. Babcock, J. O. Allen, S. Fergusson-Miller, and R. B. Gennis. 1996. Polar residues in helix VIII of subunit I of cytochrome *c* oxidase influence the activity and the structure of the active site. *Biochemistry.* 35:10776–10783.
12. Brzezinski, P., and P. Ädelroth. 1998. Proton-controlled electron transfer in cytochrome *c* oxidase: functional role of the pathways through Glu 286 and Lys 362. *Acta Physiol. Scand. Suppl.* 643:7–16.
13. Mills, D. A., and S. Ferguson-Miller. 1998. Proton uptake and release in cytochrome *c* oxidase: separate pathways in time and space? *Biochim. Biophys. Acta.* 1365:46–52.
14. Aagaard, A., G. Gilderson, D. A. Mills, S. Ferguson-Miller, and P. Brzezinski. 2000. Redesign of the proton-pumping machinery of cytochrome c oxidase: proton pumping does not require Glu(I-286). *Biochemistry.* 39:15847–15850.
15. Zaslavsky, D., and R. B. Gennis. 2000. Proton pumping by cytochrome oxidase: progress, problems and postulates. *Biochim. Biophys. Acta.* 1458:164–179.
16. Pfitzner, U., K. Hoffmeier, A. Harrenga, A. Kannt, H. Michel, E. Bamberg, O. M. Richter, and B. Ludwig. 2000. Tracing the D-pathway in reconstituted site-directed mutants of cytochrome *c* oxidase from *Paracoccus denitrificans*. *Biochemistry.* 39:6756–6762.
17. Kannt, A., C. R. D. Lancaster, and H. Michel. 1998. The coupling of electron transfer and proton translocation: electrostatic calculations on *Paracoccus denitrificans* cytochrome *c* oxidase. *Biophys. J.* 74:708–721.
18. Ma, J., P. H. Tsatsos, D. Zaslavsky, B. Barquera, J. M. Thomas, A. Katsonouri, A. Puustinen, M. Wikstrom, P. Brzezinski, J. O. Alben, and R. B. Gennis. 1999. Glutamate-89 in subunit II of cytochrome *bo*3 from *Escherichia coli* is required for the function of the heme-copper oxidase. *Biochemistry.* 38:15150–15156.
19. Bränden, M., A. Namslauer, O. Hansson, R. Aasa, and P. Brzezinski. 2003. Water-hydroxide exchange reactions at the catalytic site of heme-copper oxidases. *Biochemistry.* 42:13178–13184.
20. Riistama, S., G. Hummer, A. Puustinen, R. B. Dyer, W. H. Woodruff, and M. Wikström. 1997. Bound water in the protein translocation mechanism of the heme-copper oxidases. *FEBS Lett.* 414:275–280.
21. Pomès, R., G. Hummer, and M. Wikström. 1998. Structure and dynamics of a proton shuttle in cytochrome *c* oxidase. *Biochim. Biophys. Acta.* 1365:255–260.
22. Hofacker, I., and K. Schulten. 1998. Oxygen and proton pathways in cytochrome *c* oxidase. *Proteins.* 30:100–107.
23. Zheng, X., D. M. Medvedev, J. Swanson, and A. A. Stuchebrukhov. 2003. Computer simulation of water in cytochrome *c* oxidase. *Biochim. Biophys. Acta.* 1557:99–107.
24. Wikström, M., M. I. Verkhovsky, and G. Hummer. 2003. Water-gated mechanism of proton translocation by cytochrome *c* oxidase. *Biochim. Biophys. Acta.* 1604:61–65.
25. Olkhova, E., M. Hutter, M. A. Lill, V. Helms, and H. Michel. 2004. Dynamic water networks in cytochrome *c* oxidase from *Paracoccus denitrificans* investigated by molecular dynamics simulations. *Biophys. J.* 86:1873–1889.
26. Lancaster, C. R. D. 2003. The role of electrostatics in proton-conducting membrane protein complexes. *FEBS Lett.* 545:52–60.
27. Gilson, M. K., A. Rashin, R. Fine, and B. Honig. 1985. On the calculation of electrostatic interactions in proteins. *J. Mol. Biol.* 183: 503–516.

28. Verkhovskaya, M. L., A. Garcia-Horsman, A. Puustinen, J.-L. Rigaud, J. E. Morgan, M. I. Verkhovsky, and M. Wikström. 1997. Glutamic acid 286 in subunit I of cytochrome bo_3 is involved in proton translocation. *Proc. Natl. Acad. Sci. USA*. 94:10128–10131.

29. Popović, D. M., and A. A. Stuchebrukhov. 2004. Electrostatic study of the proton pumping mechanism in bovine heart cytochrome *c* oxidase. *J. Am. Chem. Soc*. 126:1858–1871.

30. Popović, D. M., J. Quenneville, and A. A. Stuchebrukhov. 2005. DFT/electrostatic calculations of p*Ka* values in cytochrome *c* oxidase. *J. Phys. Chem*. 109:3616–3626.

31. Olsson, M. H. M., P. K. Sharma, and A. Warshel. 2005. Simulating redox coupled proton transfer in cytochrome *c* oxidase: looking for the proton bottleneck. *FEBS Lett*. 579:2026–2034.

32. Simonson, T., and C. L. Brooks. 1996. Charge screening and the dielectric constant of proteins: insights from molecular dynamics. *J. Am. Chem. Soc*. 118:8452–8458.

33. Antosiewicz, J., J. A. McCammon, and M. K. Gilson. 1994. Prediction of pH-dependent properties of proteins. *J. Mol. Biol*. 238:415–436.

34. Antosiewicz, J., J. A. McCammon, and M. K. Gilson. 1996. The determinants of pK_as in proteins. *Biochemistry*. 35:7819–7833.

35. Antosiewicz, J., J. M. Briggs, A. H. Elcock, M. K. Gilson, and J. A. McCammon. 1996. Computing the ionization states of proteins with a detailed charge model. *J. Comput. Chem*. 17:1633–1644.

36. Demchuk, E., and R. C. Wade. 1996. Improving the continuum electrostatic approach to calculating pK_as of ionisable groups in proteins. *J. Phys. Chem*. 100:17373–17387.

37. Gunner, M. R., and E. Alexov. 2000. A pragmatic approach to structure based calculation of coupled proton and electron transfer in proteins. *Biochim. Biophys. Acta*. 1458:63–87.

38. Schutz, C. N., and A. Warshel. 2001. What are the dielectric ''constants'' of proteins and how to validate electrostatic models? *Proteins*. 44:400–417.

39. Humphrey, W., A. Dalke, and K. Schulten. 1996. VMD: visual molecular dynamics. *J. Mol. Graph*. 14:33–38.

40. Brooks, B. R., R. E. Bruccoleri, B. D. Olafson, D. J. States, S. Swaminathan, and M. Karplus. 1983. CHARMM: a program for macromolecular energy minimization and dynamics calculations. *J. Comput. Chem*. 4:187–217.

41. Berneche, S., and B. Roux. 1998. The ionisation state and the conformation of Glu-71 in the KcsA K^+ channel. *Biophys. J*. 82: 772–780.

42. MacKerell, A., Jr., J. Wiorkiewicz-Kuczera, and M. Karplus. 1995. An all-atom empirical energy function for the simulation of nucleic acids. *J. Am. Chem. Soc*. 117:11946–11975.

43. MacKerell, A. D., Jr., D. Bashford, M. Bellot, R. L. Dunbrack, J. D. Evanseck, M. J. Field, S. Fischer, J. Gao, H. Guo, D. Joseph-McCarthy, S. Ha, L. Kuchnir, et al. 1998. All-atom empirical potential for molecular modeling and dynamics studies of proteins. *J. Phys. Chem. B*. 102:3586–3616.

44. Davis, M. E., and J. A. McCammon. 1991. Dielectric boundary smoothing in finite difference solutions of the Poisson equation: an approach to improve accuracy and convergence. *J. Comput. Chem*. 12:909–912.

45. Oefner, C., A. D'Arcy, J. J. Daly, K. Gubernator, R. L. Charnas, I. Heinze, C. Hubschwerlen, and F. K. Winkler. 1990. Refined crystal structure of *b*-lactamase from *Citrobacter freundii* indicates a mechanism for *b*-lactam hydrolysis. *Nature*. 343:284–288.

46. Bashford, D., and M. Karplus. 1990. pKa's of ionisable groups in proteins: atomic detail from a continuum electrostatic model. *Biochemistry*. 29:10219–10225.

47. Yang, A. S., M. R. Gunner, R. Sampogna, K. Sharp, and B. Honig. 1993. On the calculations of pK_as in proteins. *Proteins*. 15:252–265.

48. Madura, J. D., J. M. Briggs, R. C. Wade, M. E. Davis, B. A. Luty, A. Ilin, J. Antosiewicz, M. K. Gilson, B. Bagheri, L. R. Scott, and J. A. McCammon. 1995. Electrostatics and diffusion of molecules in solution: simulations with the University of Houston Brownian Dynamics Program. *Comput. Phys. Commun*. 91:57–95.

49. Gilson, M. K. 1993. Multiple-site titration and molecular modeling: two rapid methods for computing energies and forces for ionizable groups in proteins. *Proteins*. 15:266–282.

50. Raquet, X., V. Lounnas, J. Lamotte-Brasseur, J. M. Frére, and R. C. Wade. 1997. pK_as calculations for class A *b*-lactamases: methodological and mechanistic implications. *Biophys. J*. 73:2416–2426.

51. Namslauer, A., and P. Brzezinski. 2004. Structural elements involved in electron-coupled proton transfer in cytochrome *c* oxidase. *FEBS Lett*. 567:103–110.

52. Pawate, A. S., J. Morgan, A. Namslauer, D. Mills, P. Brzezinski, S. Ferguson-Miller, and R. B. Gennis. 2002. A mutation in subunit I of cytochrome oxidase from *Rhodobacter sphaeroides* results in an increase in steady-state activity but completely eliminates proton pumping. *Biochemistry*. 41:13417–13423.

53. Budiman, K., A. Kannt, S. Lyubenova, O.-M. H. Richter, B. Ludwig, H. Michel, and F. MacMillan. 2004. Tyrosine-167: the origin of the radical species observed in the reaction of cytochrome *c* oxidase with hydrogen peroxide in *Paracoccus denitrificans*. *Biochemistry*. 43:11709–11716.

54. Riistama, S., A. Puustinen, A. Garcia-Horsman, S. Iwata, H. Michel, and M. Wikstrom. 1996. Channelling of dioxygen into the respiratory enzyme. *Biochim. Biophys. Acta*. 1275:1–4.